NASA TECHNICAL NOTE

NASA TN D-5263

VENTING OF LIQUID HYDROGEN TANKAGE

by John C. Aydelott and Charles M. Spuckler

Lewis Research Center
Cleveland, Ohio

NATIONAL AERONAUTICS AND SPACE ADMINISTRATION • WASHINGTON, D. C. • JUNE 1969

VENTING OF LIQUID HYDROGEN TANKAGE

By John C. Aydelott and Charles M. Spuckler

Lewis Research Center
Cleveland, Ohio

NATIONAL AERONAUTICS AND SPACE ADMINISTRATION

For sale by the Clearinghouse for Federal Scientific and Technical Information
Springfield, Virginia 22151 – CFSTI price $3.00

ABSTRACT

A 22-in. - (56-cm-) diameter spherical tank partially filled with liquid hydrogen was subjected to three venting tests. Two of the tests were conducted with uniform heating of the tank and the third with top heating only. The experimentally determined venting rates were compared with theoretically predicted venting rates equal to the energy input divided by the heat of vaporization. Each experimental venting rate was much less than the corresponding theoretically predicted venting rate. The difference between the theoretical and experimental results was concluded to be primarily caused by the superheating of the venting vapor, an effect that is commonly neglected in the analysis of venting cryogenic tanks.

VENTING OF LIQUID HYDROGEN TANKAGE

by John C. Aydelott and Charles M. Spuckler

Lewis Research Center

SUMMARY

A 22-inch- (56-cm-) diameter spherical tank partially filled with liquid hydrogen was subjected to three venting tests. Two of the tests were conducted with uniform heating of the tank and the third with top heating only. The experimentally determined venting rates were compared with theoretically predicted venting rates equal to the energy input divided by the heat of vaporization. Each experimental venting rate was much less than the corresponding theoretically predicted venting rate. The difference between the theoretical and experimental results was concluded to be primarily caused by the superheating of the venting vapor, an effect that is commonly neglected in the analysis of venting cryogenic tanks.

INTRODUCTION

Hydrogen is very effective for use as a rocket fuel because of the high specific impulse it produces when it is either reacted with an oxidizer or used as a heated expellant as in a nuclear rocket. However, mission planners and tank designers are confronted with problems that result from the many properties of hydrogen that set it apart from common fluids. Gaseous hydrogen has a low density, so it is practical for space missions to store hydrogen only as a liquid or as a liquid-solid mixture. Liquid and solid hydrogen have a very low equilibrium temperature, which makes it difficult to insulate a storage container sufficiently to prevent a net heat gain. Under these conditions, the pressure will rise until venting is required, with an accompanying propellant loss.

Reference 1 analyzes various types of venting systems and compares them with a system venting saturated vapor. The analysis includes the consideration of system weight, propellant loss, reliability, and feasibility. It was concluded that liquid or vapor removal followed by a throttling valve and either an internal or an external heat exchanger is the best venting system. Reference 2 compares venting saturated vapor with liquid

extraction, expansion, and then cooling of the tank with exterior coils. The results of these tests showed that at a low heat flux the mass flow rates for liquid venting and vapor venting were nearly the same. At a high heat flux, the liquid vent mass flow rate was 4 percent greater than the vapor mass flow rate. A similar conclusion was reached by the author of reference 3, who stated that the overall thermodynamic effect of extracting liquid and passing it through a throttle valve and a heat exchanger is essentially the same as venting saturated vapor. This conclusion is supported by data on venting under low gravity conditions that can be found in references 4 and 5. Reference 4 presents the results of experiments conducted in a drop tower using small tanks containing either freon or liquid hydrogen. Reference 5 presents the results of venting an orbiting Saturn SIVB stage containing liquid hydrogen. Both of these studies also show that rapid depressurization may result in entrainment of liquid in the vapor, and it was concluded that under reduced-gravity conditions approximately one ullage volume of vapor can be rapidly vented without venting liquid.

When theoretically evaluating various venting systems, it is common to assume that all systems vent saturated vapor. This assumption, however, can be misleading for real systems if the vented vapor is superheated. Additional data presented in reference 5 indicated that when a small acceleration was applied to the partially filled orbiting hydrogen tank slow continuous venting of superheated hydrogen vapor occurred. Also, data on the normal-gravity venting of a 50 000-gallon (189 000-liter) spherical liquid-hydrogen storage tank (ref. 6) indicated that the vented vapor was highly superheated.

This report presents the data obtained from three venting tests of a spherical 22-inch- (56-cm-) diameter liquid-hydrogen tank. Two of the tests were performed with uniform heating and one with top heating only. The effect of the variables, average heat-transfer rate and heating configuration, was determined. An analysis is presented which relates the rate of mass loss to the rate of energy input to a venting tank. Several simplifications are used to reduce the energy balance equation that results from the analysis to the commonly employed formula that equates the rate of energy input to the rate of mass loss times the heat of vaporization (saturated-vapor venting). The validity of the various simplifications is considered in light of the available data. It is concluded that, when liquid-hydrogen tanks are vented, superheated vapor may leave the tank, and the resulting rate of mass loss is much less than would be calculated based on saturated vapor venting.

ENERGY BALANCE ANALYSIS

The following theoretical analysis is based on the formulation for a boiloff calorim-

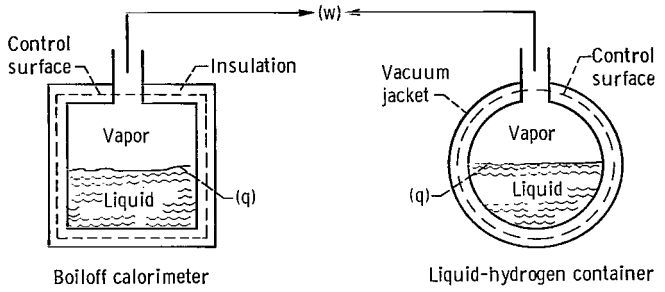

eter that is presented in reference 7. The above sketch shows the similarity between a vacuum-jacketed liquid-hydrogen container and a typical boiloff calorimeter. (Symbols are defined in appendix A.)

The following simplified equation is the first law of thermodynamics (energy balance) applied to an unsteady-flow process (ref. 8):

$$q = \frac{dU}{dt} + wh_o \tag{1}$$

$$q = \frac{d}{dt}\int_m udm + wh_o \tag{2}$$

where m, the mass within the system control surface, is

$$m = m_l + m_v + m_c \tag{3}$$

$$q = \frac{d}{dt}\int_{m_l} u_l\, dm_l + \frac{d}{dt}\int_{m_v} u_v\, dm_v + \frac{d}{dt}\int_{m_c} u_c\, dm_c + wh_o \tag{4}$$

$$q = \int_{m_l} \frac{du_l}{dt}\, dm_l + \int_{m_l} u_l \frac{d(dm_l)}{dt} + \int_{m_v} \frac{du_v}{dt}\, dm_v + \int_{m_v} u_v \frac{d(dm_v)}{dt} + \int_{m_c} \frac{du_c}{dt}\, dm_c + \int_{m_c} u_c \frac{d(dm_c)}{dt} + wh_o \tag{5}$$

The second and fourth terms on the right side of equation (5) refer only to mass transfer across the liquid-vapor interface, so the evaluation of these integrals is greatly simplified. The mass of the container is constant:

$$\left.\begin{aligned} &\frac{dm_c}{dt} = 0 \\ \text{and} \quad &\int_{m_c} u_c \frac{d(dm_c)}{dt} = 0 \end{aligned}\right\} \tag{6}$$

$$q = \int_{m_l} \frac{du_l}{dt}\, dm_l + u_{l,\,sat} \frac{dm_l}{dt} + \int_{m_v} \frac{du_v}{dt}\, dm_v + u_{v,\,sat} \frac{dm_v}{dt} + \int_{m_c} \frac{du_c}{dt}\, dm_c + wh_o \tag{7}$$

The first simplification of the energy balance results if the internal energy of the liquid is constant:

$$\left.\begin{aligned} &\frac{du_l}{dt} = 0 \\ \text{and} \quad &\int_{m_l} \frac{du_l}{dt}\, dm_l = 0 \end{aligned}\right\} \tag{8}$$

The second simplification of the energy balance results if the internal energy of the vapor is constant (inside the system control surface):

$$\left.\begin{aligned} &\frac{du_v}{dt} = 0 \\ \text{and} \quad &\int_{m_v} \frac{du_v}{dt}\, dm_v = 0 \end{aligned}\right\} \tag{9}$$

The third simplification of the energy balance results if the internal energy of the container does not change:

$$\left.\begin{aligned} &\frac{du_c}{dt} = 0 \\ \text{and} \quad &\int_{m_c} \frac{du_c}{dt}\, dm_c = 0 \end{aligned}\right\} \tag{10}$$

Applying these three simplifications to equation (7) yields

$$q = u_{l,\,sat} \frac{dm_l}{dt} + u_{v,\,sat} \frac{dm_v}{dt} + wh_o \tag{11}$$

The total mass of liquid and vapor is a constant, so the rate of change of total mass is equal to zero:

$$\frac{dm_l}{dt} + \frac{dm_v}{dt} + w = 0 \tag{12}$$

By definition,

$$\left.\begin{aligned} u_{l,\,sat} &= h_{l,\,sat} - Pv_{l,\,sat} \\ u_{v,\,sat} &= h_{v,\,sat} - Pv_{v,\,sat} \\ \lambda &= h_{v,\,sat} - h_{l,\,sat} \end{aligned}\right\} \tag{13}$$

Combining equations (11) to (13) yields

$$q = \frac{dm_v}{dt}\left[\lambda - P(v_{v,\,sat} - v_{l,\,sat})\right] + w\left[(h_o - h_{v,\,sat}) + \lambda + Pv_{l,\,sat}\right] \tag{14}$$

Assuming that the liquid and vapor are saturated and that the specific volume of the liquid and vapor vary only slightly from their average values gives

$$\frac{d\bar{v}_{v,\,sat}}{dt} = \frac{d\bar{v}_{l,\,sat}}{dt} \approx 0 \tag{15}$$

The container, occupied by the saturated liquid and vapor within the system control surface, has a constant volume:

$$m_l\bar{v}_{l,\,sat} + m_v\bar{v}_{v,\,sat} = V \tag{16}$$

Differentiating equation (16) and applying equation (15) gives

$$\frac{dm_l}{dt}\bar{v}_{l,\,sat} + \frac{dm_v}{dt}\bar{v}_{v,\,sat} = 0 \tag{17}$$

Combining equations (12) and (17) gives

$$\frac{dm_v}{dt} = \frac{w\bar{v}_{l,\,sat}}{\bar{v}_{v,\,sat} - \bar{v}_{l,\,sat}} \tag{18}$$

Combining equations (14) and (18) gives

$$q = w\lambda\left(\frac{\bar{v}_{v,\,sat}}{\bar{v}_{v,\,sat} - \bar{v}_{l,\,sat}}\right) + w(h_o - h_{v,\,sat}) \tag{19}$$

The fourth simplification of the energy balance results if saturated vapor leaves the container:

$$\left.\begin{aligned} h_o - h_{v,\,sat} &= 0 \\ \text{and} \qquad q &= w\lambda\left(\frac{\bar{v}_{v,\,sat}}{\bar{v}_{v,\,sat} - \bar{v}_{l,\,sat}}\right) \end{aligned}\right\} \tag{20}$$

This is the classical expression for boiloff calorimeter calculations. The fifth simplification of the energy balance results if the specific volume of the liquid is much smaller than the specific volume of the vapor:

$$\left.\begin{aligned} \frac{\bar{v}_{v,\,sat}}{\bar{v}_{v,\,sat} - \bar{v}_{l,\,sat}} &\approx 1 \\ \text{and} \qquad q &= w\lambda \end{aligned}\right\} \tag{21}$$

Equation (21) is the classical expression for boiler calculations, the formula that is commonly used by mission planners and tank designers to determine the rate of mass loss from venting cryogenic storage tanks. It should be remembered that equation (21) is based on five simplifications:

(1) Constant liquid internal energy
(2) Constant vapor internal energy
(3) Constant container internal energy
(4) Saturated vapor leaving the container
(5) A much smaller specific volume of the liquid than that of the vapor

The validity of these simplifications should be examined for each venting cryogenic storage tank.

APPARATUS

Liquid-Hydrogen Container

A schematic drawing of the liquid-hydrogen experimental apparatus is presented in figure 1. The apparatus consists of three concentric spheres: the inner sphere contains the liquid hydrogen, the intermediate sphere has electric heating coils mounted on its exterior surface, and the outer sphere serves as a vacuum jacket to reduce gaseous conduction of heat. The outer surface of the inner sphere and the inner surface of the heaters were painted black to increase their emissivity. The stainless-steel fill and vent tubes supported the inner sphere.

A heater controller, which basically consisted of a bridge circuit that balanced the resistance of a temperature sensor on each heater with a corresponding rheostat on the control panel, was used to maintain heater temperatures of 360°, 500°, or 560° R (200, 278, or 311 K).

An orifice in the hydrogen vent line was used to determine the mass of vapor vented. For the uniform heating test with high heater temperature, a 0.055-inch- (0.14-cm-) diameter orifice was put in the vent line. For the uniform heating test with low heater temperature and the top heating test, a 0.031-inch- (0.079-cm-) diameter orifice was put in the vent line. The orifices were chosen so that they were just large enough to maintain the maximum allowable pressure at the maximum venting condition. Calibration of the orifices over the pressure range of the vent cycle showed that the theoretical flow rates were within 1 percent of the actual flow rates.

Instrumentation

Temperature and pressure transducers measured the total system pressure, vacuum-space pressure, surface temperature of the inner sphere, heaters, and vacuum jacket and temperature at 16 locations inside the inner sphere. A thermocouple was used to measure the temperature of the vent gas at the orifice. Figure 2 shows the locations of the surface-temperature transducers on the inner sphere and the four carbon-resistor temperature rakes that were located within the inner sphere to measure the temperature of the hydrogen liquid and vapor. Figure 3 is a photograph which shows two of the carbon-resistor rakes. Prior to a test run, the resistance of any temperature transducer could be determined by using a digital ohmmeter mounted in the control panel. A very small electric current is passed through a temperature transducer to determine the resistance and thus the temperature of the transducer.

When a relatively high voltage is applied to a carbon resistor, its temperature, and

thus resistance, is quite different depending on whether or not the temperature probe is in the liquid or vapor phase. This phenomenon is due to self-heating. Exploitation of this fact, together with careful arrangement of the carbon resistors, made it possible to use the carbon resistors to determine the liquid level in the sphere prior to the start of a test.

The temperature of the vent gas was monitored on the control panel. The temperature was recorded at the start and end of each vent cycle. For the long vent cycles, the temperature was also recorded at various times during the cycles.

An ionization gage was used to measure the pressure in the vacuum space. The location of the gage and the attachment point of the two pressure transducers used to measure the pressure in the inner sphere can be seen in figure 1. A 28-volt direct-current power supply was used to operate the pressure transducers. The vacuum pressure was monitored continuously on the control panel. During a test, the 0- to 5-volt output from one of the inner-sphere pressure transducers was recorded on magnetic tape. The other pressure transducer was monitored with a digital voltmeter.

For the first 45 minutes of each test and for 5 to 15 minutes at intervals of at least 40 minutes, pressure and temperature data were recorded on magnetic tapes. A total of approximately 90 minutes of data was recorded for each test run.

A detailed description of the temperature and pressure measuring and recording systems and an analysis of the error associated with them are given in reference 9.

PROCEDURE

Prior to the assembly of the experimental apparatus, thermocouples were attached to the inner sphere, heaters, and vacuum jacket. All temperature transducers were calibrated at 139.5° R (78 K) by filling the inner sphere with liquid nitrogen and submerging it and the other two spheres in a liquid-nitrogen bath. The transducers were also calibrated at 347°, 486°, 537°, and 601° R (193, 270, 298, and 334 K) by placing the spheres in a controlled temperature chamber. After the experiment had been assembled, the inner-sphere temperature transducers were calibrated at 36.4° R (19.1 K) by filling the sphere with liquid hydrogen. Each temperature transducer bridge was calibrated by using a decade box to obtain a voltage-against-resistance plot. Prior to each test, the pressure transducers were calibrated with standard pressure gages.

Each of the calibration curves for the temperature transducers and for the bridges was curve fitted using a digital computer. The magnetic tapes for each test were fed into the digital computer along with the calibration curve fits. An automatic data reduction program returned printed temperature data at half-second intervals for each transducer. A plot of the output of the pressure transducers was obtained by feeding the out-

put of the magnetic data tape into a line recorder.

For each of the tests, the experiment was prepared in an identical manner; only the actual test conditions were varied. The space between the inner and outer spheres was evacuated first with a mechanical pump and then with a diffusion pump. Then the inner sphere was filled with liquid hydrogen. The addition of the liquid hydrogen reduced the pressure between the inner and outer spheres due to cryogenic pumping. The capillary tubes (fig. 1) were used to remove liquid from the inner sphere until the approximate desired liquid level was obtained. By recording the time when the liquid level went below each resistor and extrapolating to the starting time of the test, the initial percent filling could be determined.

Transients were eliminated by setting the heater controller to maintain the desired heater temperature prior to determining the liquid level for the test. At minus 1 minute, the system began to record data on magnetic tape. At zero time, the vent valve was closed and the experiment was allowed to self-pressurize. The tank vent was opened when the pressure reached approximately 50 psia (34.5 N/sq cm), and the tank was allowed to vent until the pressure decreased to approximately 45 psia (31.1 N/sq cm). This venting cycle was repeated until the end of the test. A stopwatch was used to obtain the length of each vent cycle.

EXPERIMENTAL RESULTS

The experiments performed consisted of two tests with uniform heating and one with top heating. A nominal initial filling of 65 percent was used for the tests. Heater temperatures of approximately 360° and 500° R (200 and 278 K) were used for the uniform heating tests. The top heating test was performed with a heater temperature of approximately 560° R (311 K).

Figures 4 to 6, showing pressure and temperature as a function of time, present the data obtained from the test runs. Each of the figures consists of four plots: (a) total pressure as a function of time, (b) upper inner-sphere temperature as a function of time, (c) middle inner-sphere temperature as a function of time, and (d) lower inner-sphere temperature as a function of time. The solid lines on the plots of temperature against time result from the continuously available data for the first 45 minutes of each test. The symbols indicate the average values obtained from the occasional bursts of recorded data; the symbols were then connected with dashed lines. Figure 7, an expanded section of some of the data presented in figure 6, shows in detail the typical variations in temperature and pressure obtained in all the tests. The experimental data presented in figures 4 and 5 (tests 1 and 2) show the effect of two different uniform heat fluxes of 23.5 and 87.5 Btu per square foot (74.1 and 275.7 W/sq m). The experimental data presented

in figure 6 (test 3) presents the effects of top heating at an average heat flux rate over the whole inner sphere of 76.1 Btu per hour per square foot (239.9 W/sq m). The heating condition for test 3 is similar to what a bare stainless-steel tank in space would experience if the top of the tank were oriented toward the sun. The total energy input rates for tests 2 and 3 were intended to be approximately the same. The heat-transfer rate for test 1 was intended to be approximately one-quarter of the heat-transfer rate for test 2.

DISCUSSION OF EXPERIMENTAL RESULTS

Energy Balance Analysis

The ANALYSIS section of this report provides a good introduction to the discussion of the experimental results. Tank designers and mission planners commonly use the highly simplified form of the venting tank energy balance which states that the heat-transfer rate is equal to the product of the mass flow rate and the heat of vaporization (eq. (21) of the ANALYSIS). It is realized that for a real cryogenic storage system the most difficult problem may be accurately determining the heat transfer rate. However, the purpose of this report is to consider the validity of applying the many simplifications to the venting tank energy balance in light of the available experimental data.

Energy Distribution

Liquid. - The first simplification that was applied to the venting tank energy balance was based on the existence of a constant liquid internal energy (eq. (8) of the ANALYSIS). This is a valid simplification only if the liquid is initially at the saturation temperature corresponding to the desired vent pressure. This point is best made by reference to figure 8 which is a plot of the average mass flow rate as a function of time for a typical venting test. The test pressure history was intended to be similar to those for a real cryogenic storage tank. The tank was filled and initially allowed to vent at atmospheric pressure. At the start of the test, the tank was sealed and self-pressurization took place until the maximum allowable pressure of 50 psia (34.5 N/sq cm) was reached. Then the vent valve was alternately opened and closed as the tank pressure cycled between 50 and 45 psia (34.5 and 31 N/sq cm). Consequently, the saturation temperature of the liquid was raised approximately 8° R (4.5 K). (The required properties of hydrogen were obtained from ref. 10.) Corresponding to this increase in temperature is an increase in the internal energy of the liquid so that during the early part of the test a large portion of the incoming energy is absorbed by the liquid. The results presented in figure 8 show

that during the self-pressurization phase the mass flow rate is zero, and then the average mass flow rate remains quite low until the liquid is heated to the new saturation temperature.

The error that will be introduced if the effect of liquid heating is not included in the analysis will depend on both the heat-transfer rate and the storage time. A knowledge of the initial mass of liquid together with the allowable change in pressure determines the heat capacity of the liquid. The product of the heat-transfer rate and the storage time yields the total energy input to the tank. If the heat capacity of the liquid is an appreciable percentage of the total energy input, the effect of liquid heating should be included in the analysis.

Of secondary interest is the rate at which the incoming energy is absorbed by the liquid. If storage times are relatively short, there may be some advantage to mechanically mixing the liquid or orienting the tank relative to the source of energy input (ref. 9). Either of these will ensure that all of the liquid is heated to the higher saturation temperature, thus minimizing the mass loss due to venting. For long storage times, the liquid will eventually absorb the same amount of energy irrespective of the rate at which it is absorbed.

Vapor. - The second simplification that was applied to the venting tank energy balance was based on the existence of a constant vapor internal energy (eq. (9) of the ANALYSIS). The data presented in figures 4(b), 5(b), and 6(b) show that large changes take place in the temperature of the vapor, especially during the self-pressurization phase and immediately following. As venting begins, the temperature of the vapor increases rapidly, absorbing energy, and then decreases rapidly, rejecting energy. For tests 1 and 2 (figs. 4(b) and 5(b)), the temperature of the vapor returns to approximately the initial condition before starting a gradual increase as venting continues. As a consequence, from the point of view of an energy balance and resulting mass loss, the effect of the early large changes in temperature of the vapor can be neglected. However, for test number 3, in particular, and for all the tests if the storage time is short, the effect of vapor heating could be important.

In general, the mass of the vapor will be quite small compared with the total mass of the system. Consequently, as the temperature of the vapor gradually increases, following the initial transient, it will absorb only a small amount of energy.

Container. - The third simplification that was applied to the venting tank energy balance was based on the existence of a constant container internal energy (eq. (10) of the ANALYSIS). The data presented in figures 4(b), 5(b), and 6(b) show that the temperature response of the container was similar to the temperature response of the vapor. For tests 1 and 2, if storage times are long, the effect of the initial transient will be cancelled out. However, for test number 3, in particular, and for all the tests, if the storage time is short, the effect of the container heating could be important. At later times

in the storage period, if the tank wall is thin, such as would be used for flight hardware, the mass of the container will be small, and it will absorb an insignificant amount of energy. However, if the container tank wall is thick, such as might be used for ground-based or high-pressure storage of cryogenics, the energy that is absorbed by the tank should be included in the analysis.

Evaluation of energy integrals. - For long storage times, evaluation of the effect of liquid heating will be fairly easy since all the liquid will be at a uniform temperature both initially and finally. Evaluation of short-storage-time liquid heating will be more difficult because the temperature will be a function of position. The same difficulty always exists for vapor and container heating. For real tank tests, many temperature transducers will be required to adequately map the temperature profiles. Once the temperature as a function of position has been determined, the specific internal energy and density of the vapor, container, or liquid can be determined at any time. For the vapor, container, or liquid, it is then necessary to determine the time rate of change of the internal energy as a function of position and evaluate the appropriate terms in the energy balance (eq. (7) of the ANALYSIS).

Fluid Properties

Specific volume. - A further simplification that was applied to the venting tank energy balance is valid if the specific volume of the liquid is much smaller than the specific volume of the vapor (eq. (21) of the ANALYSIS). For hydrogen at atmospheric pressure, the specific volume of the liquid is slightly more than 1 percent of the specific volume of the vapor, and the simplification is certainly valid. At elevated pressures, the simplification becomes less valid because the specific volume of the vapor is reduced while the specific volume of the liquid is essentially unchanged. At 50 psia (34.5 N/sq cm), the specific volume of liquid hydrogen is slightly more than $6\frac{1}{2}$ percent of the specific volume of hydrogen vapor, and appreciable error would be introduced by including the simplification. Since evaluation of the term in the energy balance involving the specific volume of the liquid and vapor is quite simple, it is recommended, at least for hydrogen storage, that the term be included.

Superheated vapor. - The simplification of the venting tank energy balance, which results if saturated vapor is assumed to leave the container, in most cases should not be applied to cryogenic storage tanks. For hydrogen at 50 psia (34.5 N/sq cm), the energy absorbed in superheating 1 pound of vapor 60° R (33 K) is approximately the same as the heat of vaporization. The data presented in figures 4(b), 5(b), and 6(b) show that, for the reported tests, the vapor leaving the venting hydrogen container (temperature transducer 25) is definitely superheated, since the saturation temperature is always less than

46° R (26 K). If the superheating of the vapor is not accounted for in any prediction of venting mass flow rates, tremendous errors may result. Figure 8 shows how the mass flow rate decreases as the temperature of the vented vapor increases after approximately 40 minutes of the test. Experimentally, only one temperature transducer, located at the outlet of the tank, is required to include the effect of superheated vapor in the analysis.

Venting Characteristics

Pressure as a function of time. - The importance of the venting vapor temperature and liquid heating can be seen by studying figures 4(a), 5(a), and 6(a) which are plots of pressure as a function of time for the three tests. Following the self-pressurization phase, the venting vapor temperature is high so that the vent cycles are short. As time progresses, the venting vapor temperature decreases, because of the generation of saturated vapor at the liquid-vapor interface, and the vent cycles become longer. Also, immediately following the self-pressurization phase, the liquid is absorbing a large percentage of the incoming energy so that there is less energy that must be dissipated by venting. For tests 1 and 2, uniform heating (figs. 4(b) and (d) and 5(b) and (d)), the liquid temperature reaches a maximum at approximately the same time that the venting vapor temperature reaches a minimum, and a much longer vent cycle results (figs. 4(a) and 5(a)). During this continuous venting period, the venting vapor temperature slowly increases, because of the dropping liquid-vapor interface, until intermittent venting is again capable of keeping the tank pressure below 50 psia (34.5 N/sq cm). In the case of test 3, top heating (figs. 6(b) and (d)), the venting vapor temperature reaches a minimum first, and a continuous venting period begins (fig. 6(a)). The venting vapor temperature increases until a period of intermittent venting results. Since the tank is being heated only from the top, it takes much longer for the liquid temperature to reach a maximum. When the liquid has absorbed all the energy it can, another continuous vent cycle follows. Finally, the venting vapor temperature increases, as the liquid-vapor interface drops, so that intermittent venting is again possible, and the pressure curve is similar to that of the first two tests.

Mass loss as a function of heat input. - The experimental results obtained from the three tests were compared by determining both the rate of heat input to the tank and the rate at which mass left the tank. The heat input to a real tank was obtained by performing a heat-transfer analysis. Appendix B contains the details of the heat-transfer analysis used for this experimental program. The results of this analysis indicated that the main source of energy input to the experiment was radiant exchange from the heaters. Heat transfer due to conduction along the fill tube, vent tube, and instrumentation wires and gaseous conduction through the vacuum space was less than 1 percent of the total en-

ergy input. An orifice was used to measure the rate at which mass left the hydrogen container during venting. The pressure upstream of the orifice was always great enough to cause choked-flow conditions to exist at the throat of the orifice. Consequently, the mass flow equation for choked flow from reference 11 (different symbols have been used) was used to determine the mass of vapor vented:

$$w = \frac{AP_T}{(T_T)^{1/2}}\left[\frac{\gamma M}{R}\left(\frac{2}{\gamma+1}\right)^{(\gamma+1)/(\gamma-1)}\right]^{1/2}$$

Both the total heat input and the total mass vented were determined as a function of time and cross plotted in figure 9, which is a plot of the mass vented as a function of heat input. The theoretical line that appears in this figure is based on a homogeneous pressure rise from 15 to 50 psia (10.5 to 34.5 N/sq cm) followed by a mass loss equal to the heat input divided by the heat of vaporization (eq. (21) of the ANALYSIS section).

Reference 9 discusses the self-pressurization phase of the tests in some detail for a similar tank. For the purposes of this report, it is of interest only to note that the first vent cycle is necessary sooner for the real tanks than for the theoretical model and that heating from the top causes even greater rates of pressure rise and earlier venting. However, the results presented in figure 9 show that only for very short test times is there an advantage to maintaining homogeneous conditions in the tank. As was discussed in the Energy Distribution section, this result is due to the fact that under real test conditions the liquid absorbs energy at a slower rate than would be predicted by the homogeneous model. But soon after venting is started, the liquid becomes saturated at the venting pressure, and all the heat capacity of the liquid has been used.

Effect of heat-transfer rate. - The test results of the two uniformly heated tanks presented in figure 9 show that the mass loss predicted by the simple theoretical model is approximately twice as great as the actual mass loss. As the test proceeded, the rate of mass loss decreased as compared with the constant rate predicted by the simplified theoretical model. The large difference between theoretical and actual venting losses is primarily the result of the superheating of the vapor. Since the venting vapor temperature continues to increase as the test proceeds (liquid level drops), the rate of mass loss decreases.

Comparison of the two uniform heating tests shows that there was a slight decrease in mass loss, for the same total energy input, with increasing heat transfer rate. This decrease is a result of the higher venting vapor temperature that is caused by the heat being supplied to the vapor faster than the internal heat and mass transfer processes can distribute it.

Effect of heating distribution. - The effect of superheating the venting vapor is even

more dramatically displayed by the results of the top heating test. Early in the test, the mass loss predicted by the simplified theoretical model is approximately six times as great as the actual mass loss, and the ratio continues to increase as the test progresses. The top heating test has approximately the same average heat-transfer rate as uniform heating test 2, and, yet, the venting mass loss has been reduced by a factor of 3. Once again, this is a result of the higher venting vapor temperature that is caused by the heat being supplied to the vapor faster than the internal heat and mass transfer processes can distribute it.

The results of the top heating test indicate that space vehicle designers in particular should consider the orientation of hydrogen storage tanks relative to the major source of energy input, probably the sun. If the mission cannot be accomplished without venting the tank, the vehicle should be oriented so that the vapor space is facing the sun. If it is deemed desirable to so orient the vehicle, the designer should also consider the use of shadow shields that are cooled by the venting vapor. This cooling of the shields will maximize the enthalpy of the vapor that is finally dumped to space and thus minimize the total loss of the stored cryogenic fluid.

Effect of size. - It is realized that real tanks designed for the long-term storage of liquid hydrogen must have much lower average heat-transfer rates than those used in this test program. The lower heat-transfer rates will be necessary for liquid to be available at the end of the storage period. The test results presented in this report indicate that, as the heat-transfer rate is reduced, the vented vapor temperature is reduced and that the experimental results more nearly approximate the simplified theoretical model. However, it is also probable that much larger tanks than the reported test tank will be used. The fact that the vented vapor temperature increased as the liquid level in the tank dropped indicates that the vented vapor temperature would also increase as the tank size was increased.

Reference 6 presents data on the normal-gravity venting of a 50 000-gallon (189 000-liter) spherical liquid-hydrogen storage tank. The average uniform heat-transfer rate was approximately 0.6 Btu per hour per square foot (1.9 W/sq m), and yet the temperature of the vented vapor was 119° R (66 K). The rate of mass loss is still only about half as great as the simplified theoretical model predicts. Consequently, the effects of increased size and reduced heat-transfer rate may counteract each other.

Effect of gravity. - Although of limited value, the test data presented in reference 5 show that superheated vapor was vented from an orbiting Saturn SIVB stage. A precise determination of either the average heat-transfer rate or the heating configuration from the available data is difficult. The fact that superheated vapor at a temperature as high as 240° R (133 K) did leave the tank is significant. This occurred during the continuous vent cycle when the vented gas was used to provide thrust that kept the liquid settled in the bottom of the tank.

The authors believe that the effect of the acceleration level on the liquid configuration in orbiting tanks or deep space probes may be more important than the effect of the acceleration level on the heat- and mass-transfer processes within the tank. The liquid configuration will determine how far the liquid-vapor interface is from the tank vent and, thus, the degree of superheat attained by the vapor. Consequently, vehicle designers will have to consider the advantages of venting superheated gas, thus conserving the most propellant, against the disadvantages of including thrusters or baffles to position the liquid.

SUMMARY OF RESULTS

A 22-inch- (56-cm-) diameter spherical tank partially filled with liquid hydrogen was subjected to three venting tests. The tank was subjected to two uniform heating tests with different heat-transfer rates and to one test with only top heating. The tank vent was opened when the pressure reached approximately 50 psia (34 N/sq cm), and the tank was allowed to vent until the pressure decreased to approximately 45 psia (31 N/sq cm). The data from the tests and the presented analysis were used to determine the mass vented from the tank as a function of the energy input. The experimentally determined venting rates were compared with theoretically predicted venting rates equal to the energy input divided by the heat of vaporization (saturated-vapor venting). The following results were obtained:

1. For all the tests, the vented vapor was superheated so that the mass vented was much less than that if saturated vapor had left the tank.

2. The amount of vapor superheat was affected most by the heating configuration. The mass vented during the top heating test was approximately one-sixth the mass loss that would have resulted if saturated vapor had left the tank.

3. The mass loss during the uniform heating tests was approximately one-half the mass loss that would have resulted if saturated vapor had left the tank.

4. The mass vented as a function of energy input decreased slightly as the heat-transfer rate was increased.

Lewis Research Center,
National Aeronautics and Space Administration,
Cleveland, Ohio, February 25, 1969,
124-09-17-01-22.

APPENDIX A

SYMBOLS

A	surface area, sq ft; sq m
a	accommodation coefficient
$B_{j,1}$	absorption factor
C_p	specific heat, Btu/(lb)(^oR); J/(kg)(K)
F	angle factor
h	enthalpy, Btu/lb; J/kg
k	thermal conductivity, Btu/(hr)(ft)(^oR); W/(m)(K)
L	length, ft; m
M	molecular weight
m	mass, lb; kg
P	pressure, lb/sq in. abs; N/sq cm
Q	heat added, Btu; J
q	heat transfer rate, Btu/hr; W
R	universal gas constant, 1.986 Btu/(lb-mole)(^oR); 8.3143 J/(mole)(K)
r	reflectivity
T	absolute temperature, ^oR; K
t	time, hr
U	total internal energy, Btu; J
u	specific internal energy, Btu/lb; J/kg
V	volume, cu ft; cu m
v	specific volume, cu ft/lb; cu m/kg
$\bar{v}$	average specific volume, cu ft/lb; cu m/kg
w	mass flow rate, lbm/hr; kg/hr
x	linear distance, ft; m
γ	ratio of specific heats, C_p/C_v
ϵ	emissivity
λ	heat of vaporization, Btu/lb; J/kg
ρ	density, lb/cu ft; kg/cu m
σ	Stefan-Boltzmann constant, 0.1713×10^{-8} Btu/(hr)(sq ft)($^oR^4$); 5.6697×10^{-8} W/(sq m)(K^4)

Subscripts:

a	absorbed
c	container
gc	gaseous conduction
j	summation variable
L	at x = L
ℓ	liquid
m	mean or average value
n	summation variable
o	vented vapor
r	radiant
rr	reradiated
sat	saturation
sc	solid conduction
st	stored

T	total
v	vapor
vg	at vacuum gage
w	wall
0	at x = 0
1	inner sphere
2	upper heater
3	lower heater
4	opening in upper heater
5	combined upper and lower heaters
6	outer sphere

APPENDIX B

HEAT-TRANSFER ANALYSIS

The amount of energy absorbed by the contained hydrogen is equal to the heat transferred to the sphere by radiation, solid conduction, and gaseous conduction minus the amount of energy stored in the container itself; that is,

$$Q_a = (q_r + q_{sc} + q_{gc})\Delta t - Q_{st} \tag{B1}$$

The amount of heat transferred by thermal radiation from the heated intermediate sphere to the inner sphere is determined by the method presented in reference 12. For the radiant exchange calculations, the outside of the inner sphere is assigned the number 1; the inside of the upper heater, number 2; the inside of the lower heater, number 3; and the opening in the upper heater, number 4. The net rate of radiant heat absorbed by the inner sphere when both heaters are installed is

$$q_1 = \sum_{j=1}^{4} \sigma B_{j,1} \epsilon_j A_j T_j^4 - \sigma \epsilon_1 A_1 T_1^4 \tag{B2}$$

where $B_{j,1}$, the absorption factor, is defined as the fraction of the total radiant-energy emission of surface j which is absorbed by surface 1. The absorption factors are determined by solution of the following simultaneous equations:

$$(F_{11}r_1 - 1)B_{11} + F_{12}r_2B_{21} + F_{13}r_3B_{31} + F_{11}\epsilon_1 = 0 \tag{B3}$$

$$F_{21}r_1B_{11} + (F_{22}r_2 - 1)B_{21} + F_{23}r_3B_{31} + F_{21}\epsilon_1 = 0 \tag{B4}$$

$$F_{31}r_1B_{11} + F_{32}r_2B_{21} + (F_{33}r_3 - 1)B_{31} + F_{31}\epsilon_1 = 0 \tag{B5}$$

$$F_{41}r_1B_{11} + F_{42}r_2B_{21} + F_{43}r_3B_{31} + (F_{44}r_4 - 1)B_{41} + F_{41}\epsilon_1 = 0 \tag{B6}$$

This technique treats all diffuse-radiation circumstances and requires only a knowledge of the geometry of the four surfaces, the average temperature of the surfaces, and the emissivity of the surfaces. Lewis Research Center personnel experimentally obtained the emissivity of the inner surface of the heaters and the outer surface of the hydrogen container (fig. 10) by using a sample identical to both surfaces. Because of the

wires and tubes coming through the hole in the upper heater, the heat radiated through the hole from the outer sphere was assumed to be emitted from a blackbody. When the bottom hemispherical heater was removed to obtain top heating, the outer-sphere, surface 6, had to be substituted for the removed heater, surface 3, in equation (B2) and in subsequent calculations. The inside of the outer sphere and the outside of the heaters were gold plated. The analysis was nearly insensitive to the value of emissivity for these surfaces, so an approximate value of 0.10 was assumed.

Because of the variation in temperature of the inner sphere, the last term in equation (B2) was expressed as an integral and called the inner-sphere reradiated heat flux

$$q_{1,rr} = \int_{A_1} \sigma \epsilon T^4 \, dA \tag{B7}$$

where A_1 is the surface area of the inner sphere. This integral was approximated by the summation

$$q_{1,rr} \approx \sum_{j=1}^{n} \sigma \epsilon_j T_j^4 A_j \tag{B8}$$

The hydrogen temperature profiles were assumed to be symmetric with respect to the vertical axis. In other words, at any time during a test, all vertical planes passing through the center of the inner sphere would exhibit identical temperature patterns, and the left side of such a plane would be the mirror image of the right side. This assumption is based on the fact that the inner sphere, heaters, fill and vent tubes, instrumentation wires, and liquid-vapor interface all have symmetry with respect to the vertical axis; consequently, there is no reason to anticipate that the hydrogen temperature profiles would be different on opposite sides of the container. Based on this assumption, horizontal uniform temperature sections could be used to divide the sphere into elemental surface areas. A digital computer was used to fit the curve of the emissivity as a function of temperature and the inner sphere temperature as a function of position for each time interval. An average temperature for each elemental area was used to determine the local emissivity, and the summation was performed every 30 seconds by using a digital computer.

The energy stored in the container at any time interval was also expressed as an integral

$$Q_{st} = \int_{V_{1,w}} \rho C_p T \, dV \tag{B9}$$

where $V_{1,w}$ is the volume of the container wall. This integral was approximated by the summation

$$Q_{st} \approx \sum_{j=1}^{n} \rho C_{p,j} T_j \Delta V_j \tag{B10}$$

With the same temperature distribution assumed, a digital computer was used to fit the curve of the stainless-steel specific heat as a function of temperature (found in fig. 11, data from ref. 13) and the curves of the inner-sphere temperature as a function of position for each time interval. An average temperature for each elemental volume was used to determine the specific heat, and the summation was performed every 30 seconds by using a digital computer.

The differential equation and boundary conditions for one-dimensional heat transfer by solid conduction are

$$\frac{d}{dx}\left(k \frac{dt}{dx}\right) = 0 \left\{ \begin{array}{l} \text{at } x = 0, \ T = T_0 \\ \\ \text{at } x = L, \ T = T_L \end{array} \right\} \tag{B11}$$

At the very low temperatures encountered with the use of liquid hydrogen, the thermal conductivity of most materials is highly temperature dependent and can be expressed as some function of the absolute temperature. Substituting the boundary conditions in equation (B11) and integrating (ref. 12) result in

$$\frac{q_{sc}}{A} = k_m \frac{T_0 - T_L}{L} \tag{B12}$$

where

$$k_m = \frac{1}{T_L - T_0} \int_{T_0}^{T_L} k(T) dT \tag{B13}$$

Figure 12 shows the stainless-steel thermal conductivity as a function of temperature (ref. 13) and the curve fit that was used to perform the necessary integration in equation (B13).

The amount of heat transferred through the vacuum space by gaseous conduction was

determined by the following equation (ref. 13):

$$\frac{q_{gc}}{A_1} = \frac{1}{2}\left[\frac{a_1 a_5}{a_5 + a_1(1 - a_5)\frac{A_1}{A_5}}\right]\left[\frac{\gamma + 1}{\gamma - 1}\right] \sqrt{\frac{R}{2\pi}} \frac{P}{\sqrt{T_{vg} M}} (T_5 - T_1) \tag{B14}$$

The accommodation coefficients were also obtained from reference 13.

REFERENCES

1. Mitchell, R. C.; Stark, J. A.; and White, R. C.: Zero-G Hydrogen Tank Venting Systems. Advances in Cryogenic Engineering. Vol. 12. K. D. Timmerhaus, ed., Plenum Press, 1967, pp. 72-81.

2. Warren, R. P.; and Anderson, J. W.: A System for Venting a Propellant Tank in the Absence of Gravity. Advances in Cryogenic Engineering. Vol. 12. K. D. Timmerhaus, ed., Plenum Press, 1967, pp. 63-71.

3. Allgeier, R. K.: Subcritical Cryogenic Storage Development and Flight Test. NASA TN D-4293, 1968.

4. Larkin, Bert K.; and Bowman, T. E.: The Venting of Saturated Liquids in Zero Gravity. Proceedings of the 13th Annual Technical Meeting of the Institute of Environmental Sciences, vol. 2, 1967, pp. 591-598.

5. Navickas, J.; and Madsen, R. A.: Propellant Behavior During Venting in an Orbiting Saturn S-IVB Stage. Advances in Cryogenic Engineering. Vol. 13. K. D. Timmerhaus, ed., Plenum Press, 1968, pp. 188-198.

6. Liebenberg, D. H.; and Edeskuty, F. J.: Pressurization Analysis of a Large-Scale Liquid-Hydrogen Dewar. International Advances in Cryogenic Engineering. Vol. 10. K. D. Timmerhaus, ed., Plenum Press, 1965, pp. 284-289.

7. Jacobs, R. B.: Theory of Boil-Off Calorimetry. Rev. Sci. Instr., vol. 35, no. 7, July 1964, pp. 828-832.

8. Mackey, C. O.; Barnard, W. N.; and Ellenwood, F. O.: Engineering Thermodynamics. John Wiley & Sons, Inc., 1957.

9. Aydelott, John C.: Normal Gravity Self-Pressurization of 9-Inch- (23 cm) Diameter Spherical Liquid Hydrogen Tankage. NASA TN D-4171, 1967.

10. Roder, Hans M.; and Goodwin, Robert D.: Extended Tables of Provisional Thermodynamic Functions for Para-Hydrogen (British Units); in Liquid, Fluid and Gaseous States at Pressures to 5000 PSI., 36° to 180° R and at Pressures to 1500 psia., 140° to 540° R. Rep. 7220, National Bureau of Standards, Jan. 3, 1962.

11. Shapiro, Ascher H.: The Dynamics and Thermodynamics of Compressible Fluid Flow. Vol. 1. The Ronald Press Co., 1953.

12. Gebhart, Benjamin: Heat Transfer. McGraw-Hill Book Co., Inc., 1961.

13. Scott, Russel B.: Cryogenic Engineering. D. Van Nostrand Co., Inc., 1959.

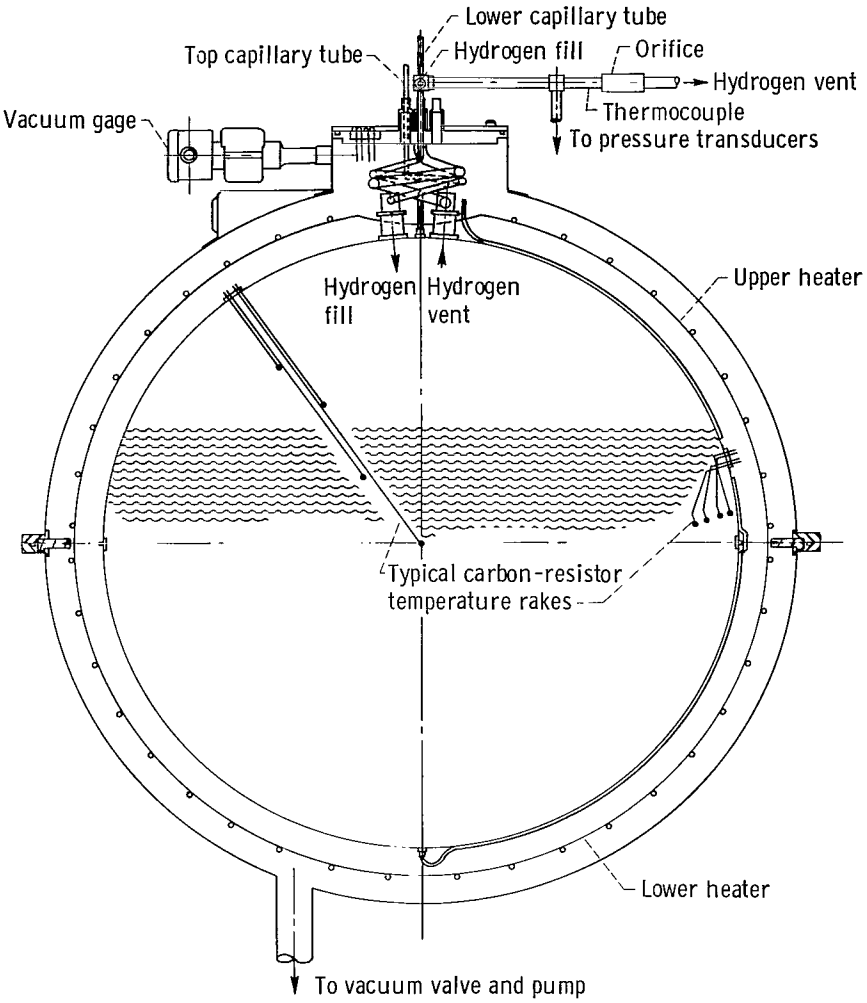

Figure 1. - Liquid-hydrogen experimental apparatus.

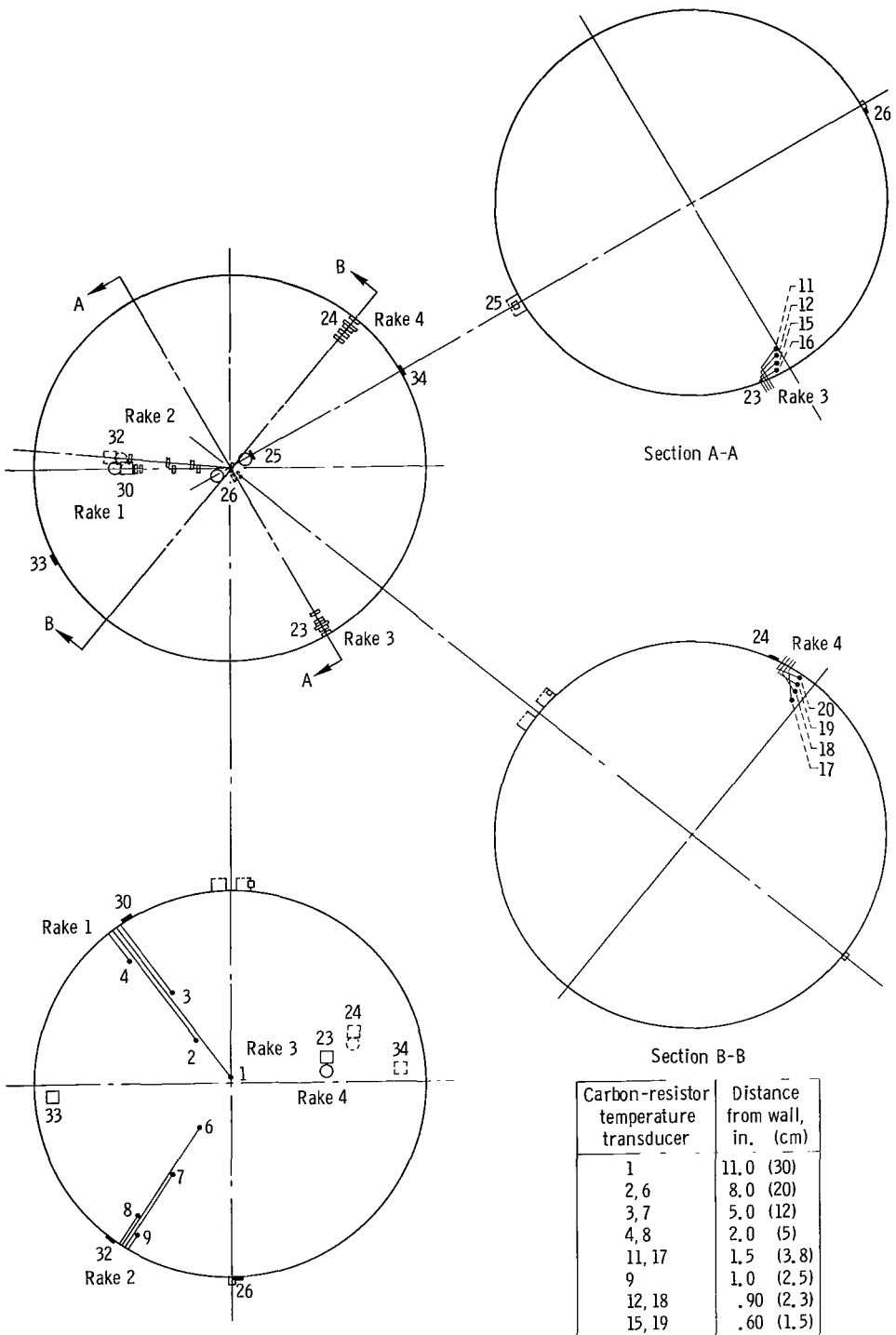

Carbon-resistor temperature transducer	Distance from wall, in. (cm)
1	11.0 (30)
2, 6	8.0 (20)
3, 7	5.0 (12)
4, 8	2.0 (5)
11, 17	1.5 (3.8)
9	1.0 (2.5)
12, 18	.90 (2.3)
15, 19	.60 (1.5)
16, 20	.20 (.5)

Figure 2. - Inner-sphere temperature transducer locations. Surface-temperature transducer locations 23, 24, 25, 26, 30, 32, 33, and 34 shown in drawing.

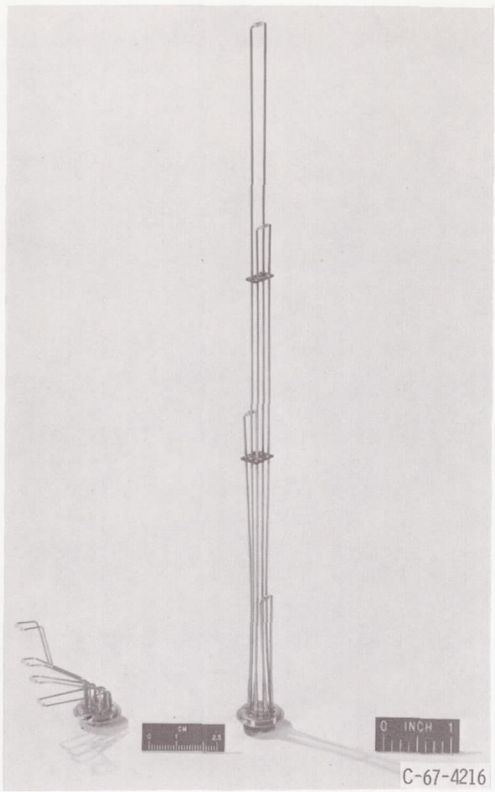

Figure 3. - Carbon-resistor rakes.

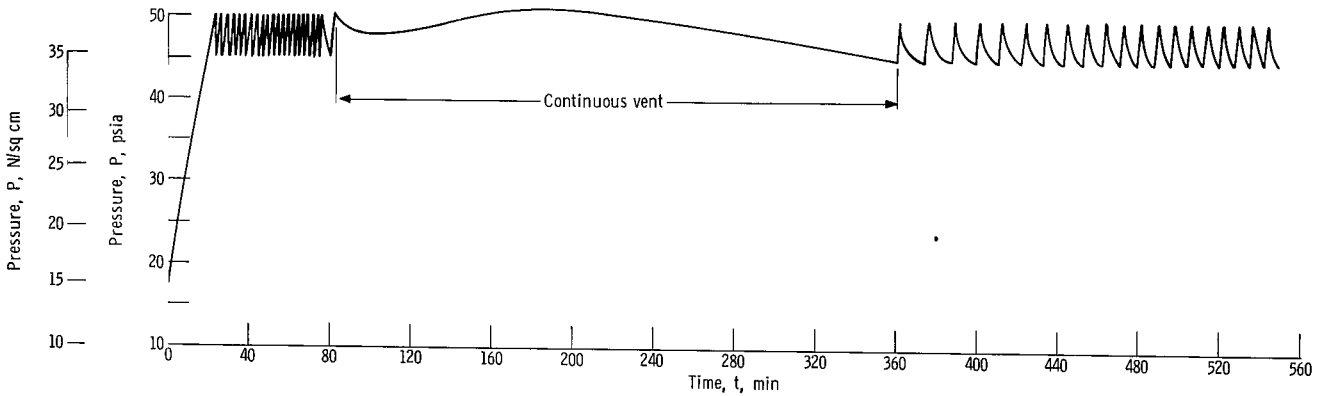

(a) Pressure as function of time.

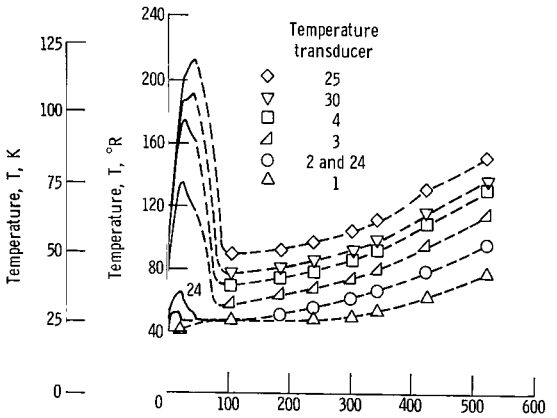

(b) Upper inner-sphere temperature as function of time. Temperature transducers 25, 30, and 24 located on outer surface.

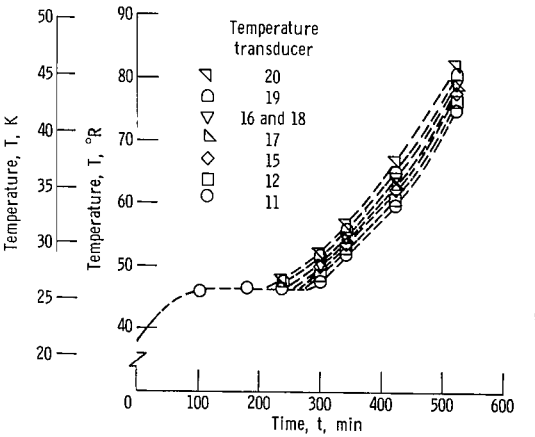

(c) Middle inner-sphere temperature as function of time.

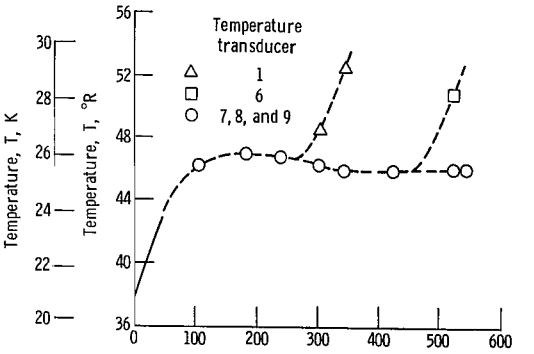

(d) Lower inner-sphere temperature as function of time.

Figure 4. - Results of uniform heating for test 1. Average heat flux, 23.5 Btu per hour per square foot (74.1 W/sq m).

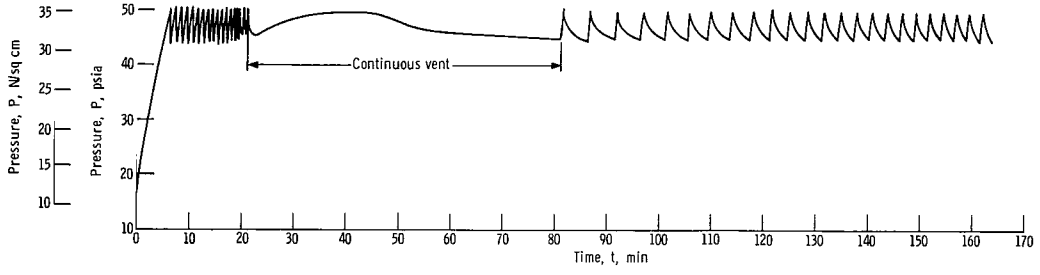

(a) Pressure as function of time.

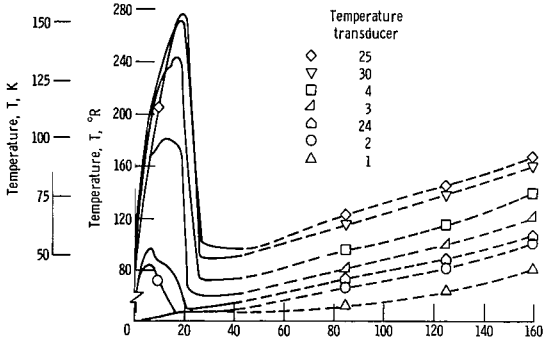

(b) Upper inner-sphere temperature as function of time. Temperature transducers 25, 30, and 24 located on outer surface.

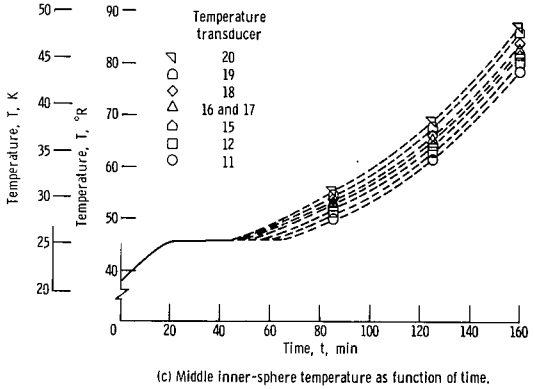

(c) Middle inner-sphere temperature as function of time.

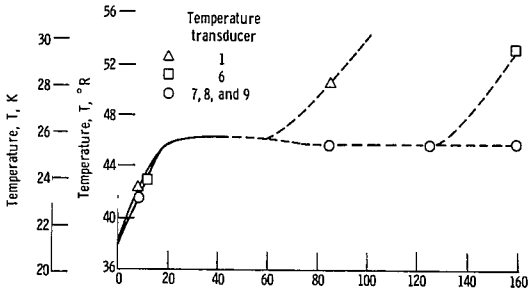

(d) Lower inner-sphere temperature as function of time.

Figure 5. - Results of uniform heating for test 2. Average heat flux, 85.5 Btu per hour per square foot (275.7 W/sq m).

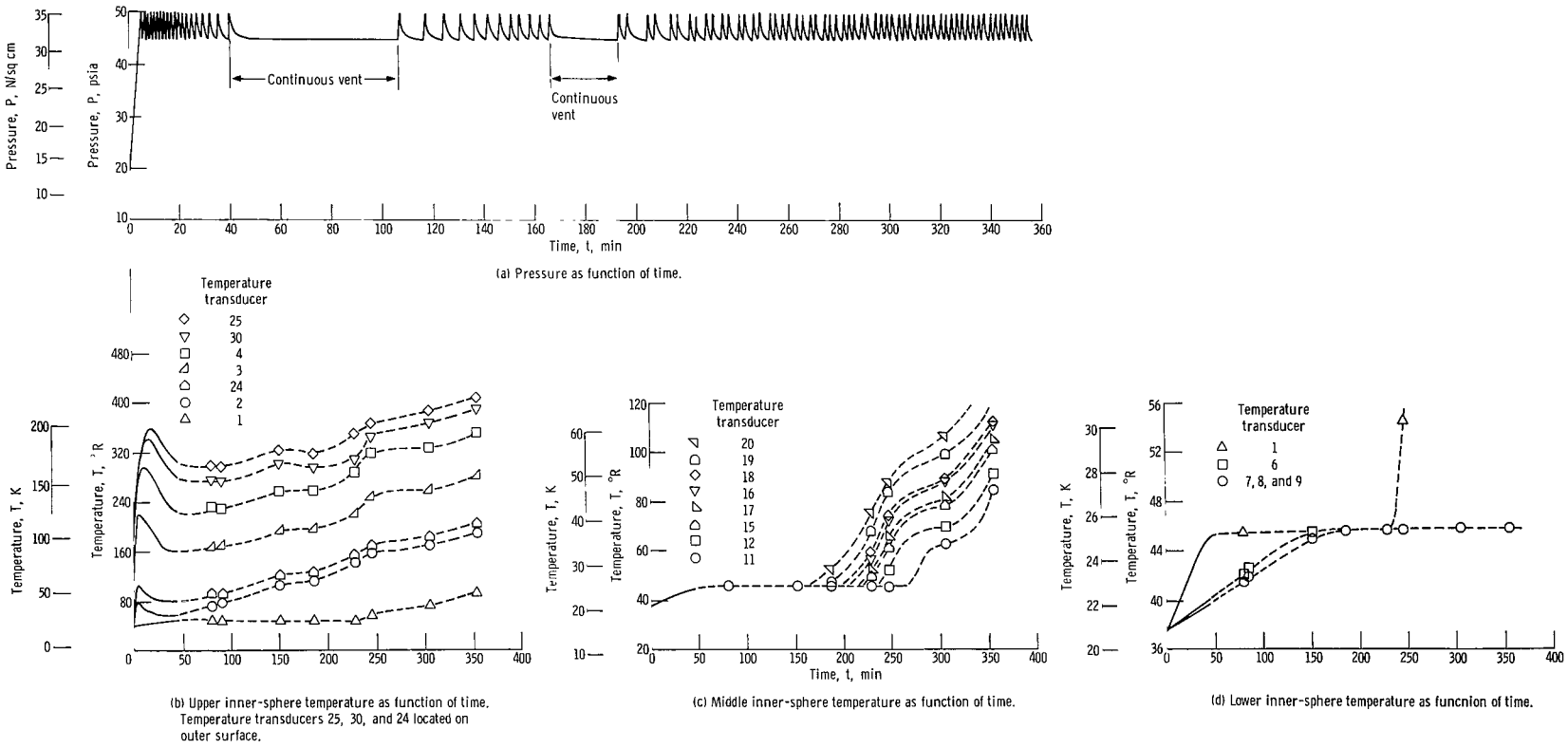

(a) Pressure as function of time.

(b) Upper inner-sphere temperature as function of time. Temperature transducers 25, 30, and 24 located on outer surface.

(c) Middle inner-sphere temperature as function of time.

(d) Lower inner-sphere temperature as funcnion of time.

Figure 6. - Results of top heating for test 3. Average heat flux, 76.1 Btu per hour per square foot (239.9 W/sq m).

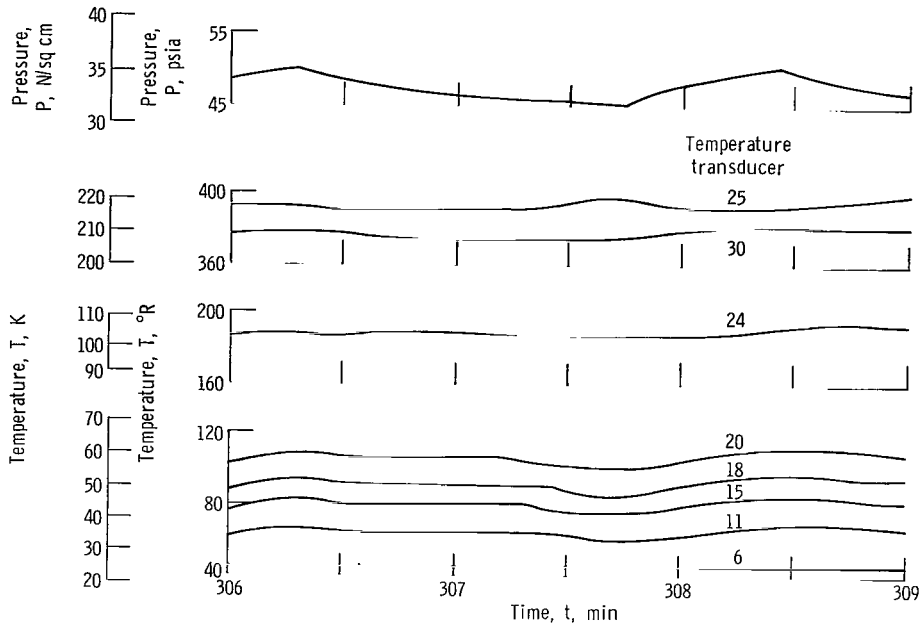

Figure 7. - Typical detailed pressure and temperature as function of time for test 3.

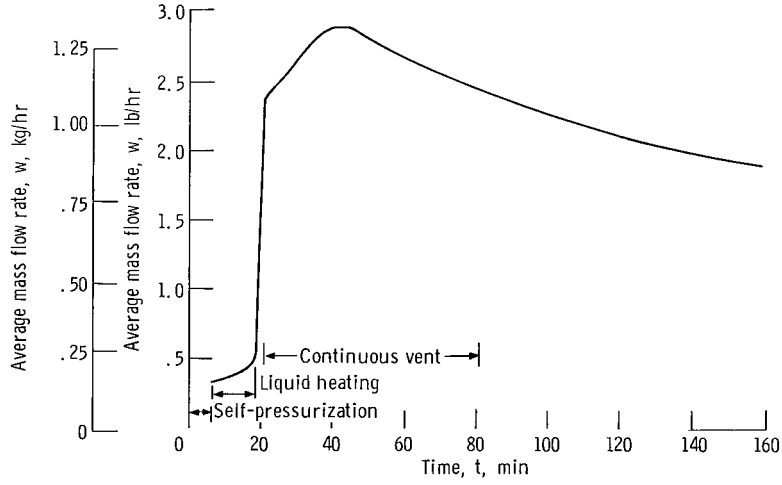

Figure 8. - Average mass flow rate as function of time for test 2.

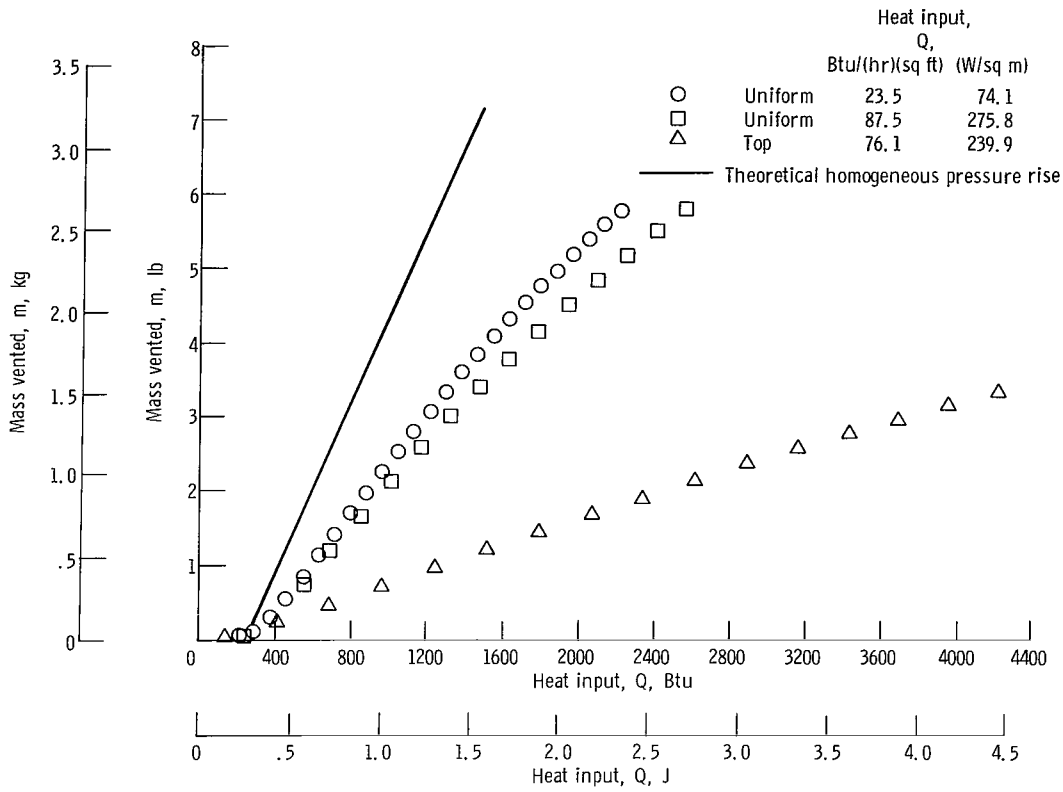

Figure 9. - Mass vented as function of heat input.

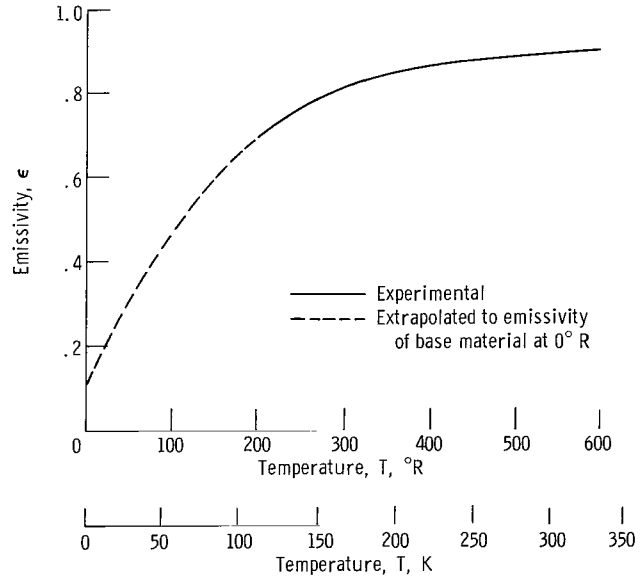

Figure 10. - Inner sphere and heater emissivity as function of temperature.

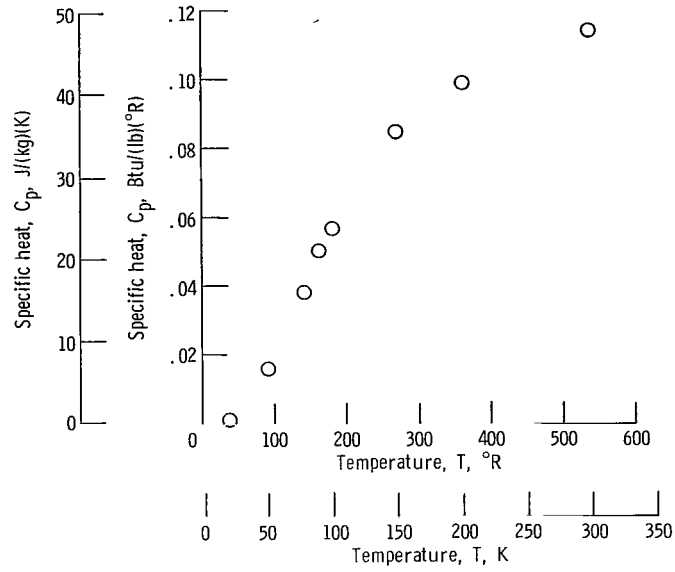

Figure 11. - Stainless-steel specific heat as function of temperature. (Data from ref. 13).

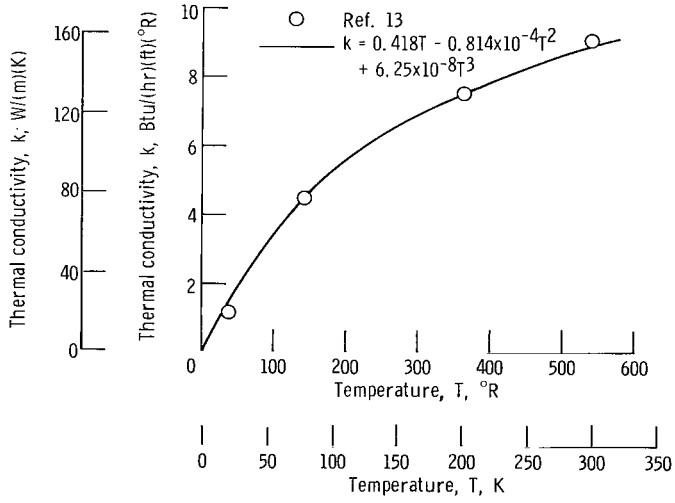

Figure 12. - Stainless-steel thermal conductivity as function of temperature.

NATIONAL AERONAUTICS AND SPACE ADMINISTRATION
WASHINGTON, D. C. 20546

OFFICIAL BUSINESS

FIRST CLASS MAIL

POSTAGE AND FEES PAID
NATIONAL AERONAUTICS AND
SPACE ADMINISTRATION

"The aeronautical and space activities of the United States shall be conducted so as to contribute . . . to the expansion of human knowledge of phenomena in the atmosphere and space. The Administration shall provide for the widest practicable and appropriate dissemination of information concerning its activities and the results thereof."

—NATIONAL AERONAUTICS AND SPACE ACT OF 1958

NASA SCIENTIFIC AND TECHNICAL PUBLICATIONS

TECHNICAL REPORTS: Scientific and technical information considered important, complete, and a lasting contribution to existing knowledge.

TECHNICAL NOTES: Information less broad in scope but nevertheless of importance as a contribution to existing knowledge.

TECHNICAL MEMORANDUMS: Information receiving limited distribution because of preliminary data, security classification, or other reasons.

CONTRACTOR REPORTS: Scientific and technical information generated under a NASA contract or grant and considered an important contribution to existing knowledge.

TECHNICAL TRANSLATIONS: Information published in a foreign language considered to merit NASA distribution in English.

SPECIAL PUBLICATIONS: Information derived from or of value to NASA activities. Publications include conference proceedings, monographs, data compilations, handbooks, sourcebooks, and special bibliographies.

TECHNOLOGY UTILIZATION PUBLICATIONS: Information on technology used by NASA that may be of particular interest in commercial and other non-aerospace applications. Publications include Tech Briefs, Technology Utilization Reports and Notes, and Technology Surveys.

Details on the availability of these publications may be obtained from:

SCIENTIFIC AND TECHNICAL INFORMATION DIVISION

NATIONAL AERONAUTICS AND SPACE ADMINISTRATION

Washington, D.C. 20546